Asian Journal of Chemistry; Vol. 34, No. 12 (2022), 3327-3332

ASIAN JOURNAL OF CHEMISTRY

https://doi.org/10.14233/ajchem.2022.23958

Phase and Electrical Properties of Rice Husk Silica-based Na_2FeSiO_4 Precursors Sintered at High Temperature

AGUS RIYANTO*, REZEKI SOFI KARIMAH, ERASRI YUNI SUHESTI, NOVITA SARI and SRI WAHYU SUCIYATI

Department of Physics, Universitas Lampung, Bandar Lampung, Indonesia

*Corresponding author: Fax: +62 721 702767; Tel: +62 721 701609; E-mail: agus.riyanto@fmipa.unila.ac.id

Received: 8 June 2022; *Accepted*: 25 October 2022; *Published online*: 25 November 2022; AJC-21064

The aim of this work is to characterize the phase and electrical properties of Na_2FeSiO_4 precursor synthesized by the sol-gel technique and then sintering with a holding period of 10 h. The FTIR analysis indicates the presence of Na-O, Fe-O, Si-O and Si-O-Si groups. Their phases were analyzed using XRD coupled with qualitative and quantitative analysis. Meanwhile, the electrical properties were characterized using UV-Vis DRS and LCR meter. The phase analysis revealed that the samples were dominated by SiO_2 and Na_2FeSiO_4 and were followed by Fe_2O_3, Fe_2SiO_4 and Na_2SiO_3. There was no substantial differences in phase composition over the sintering temperature range of 805-815 ºC. However, the volume of cell units in each phase increased gradually with an increase in sintering temperature and was followed by the increasing electrical conductivity of the samples.

Keywords: Electrical properties, Na_2FeSiO_4, Phase, Rice husk silica, Sintering.

INTRODUCTION

In the rechargeable battery systems, Li_2FeSiO_4 compound has been suggested as a cathode candidate. This compound is prepared by combining the tetrahedral structure of LiO_4, FeO_4 and SiO_4 in a specific configuration depending on its crystal system [1]. It has a stable structure and can theoretically reach a specific capacity of about 330 $mAhg^{-1}$ if used for a cathode in a Li-ion battery system [2]. However, recently, Li_2FeSiO_4 compounds are considered less competitive to be promoted as cathodes because of their low electrical conductivity and lack of lithium abundance in nature [3]. Several approaches have been made to overcome this problem. Replacing the element lithium in the Li_2FeSiO_4 compound with sodium to form a Na_2FeSiO_4 compound is one of the attractive approaches [4]. Sodium's choice substitutes Li, since Na is much more abundant than Li in nature. Although, theoretically, Na_2FeSiO_4 only produces a specific capacity of about 278 $mAhg^{-1}$, smaller than Li_2FeSiO_4 [5]. However, its electrical conductivity and ionic conductivity are more excellent than Li_2FeSiO_4 compounds [6]. This character allows Na_2FeSiO_4 to be used directly as a cathode material without adding other materials to increase its conductivity. Based on these factors, the researchers believe that Na_2FeSiO_4 has the potential to become a cathode material in rechargeable battery systems.

Several methods have been successfully applied to produce Na_2FeSiO_4 compounds, including solvothermal, solid-state reaction and sol-gel methods [6-10]. Kee *et al.* [7] succeeded in obtaining the Na_2FeSiO_4 compounds by applying the solvothermal method. This process produces Na_2FeSiO_4, which is accompanied by secondary phases such as Na_2SiO_3 and Fe_3O_4, however, The disadvantage of this method is that it takes a long time. Meanwhile, Kaliyappan & Chen [8] successfully prepared Na_2FeSiO_4 using the solid-state reaction method. This process produced a sample with the main phase Na_2FeSiO_4 and secondary phases such as Na_2SiO_3 and Fe_3O_4. Again, as usual, the disadvantage of this reaction approach is that it requires a high temperature; nevertheless, the reaction happens swiftly. Besides that the product produced has a relatively low homogeneity. Meanwhile, Feng *et al.* [9] reported that relatively high purity Na_2FeSiO_4 compounds might be created using the sol-gel route followed by thermal passing for 9 h at 600 ºC. In another study, Guan *et al.* [10] successfully prepared Na_2FeSiO_4 from $FeC_2O_4{\cdot}2H_2O$, CH_3COONa, TEOS, citric acid and ethanol

by applying the sol-gel method followed by a thermal process for 8 h at 600 ºC. In these studies, it was also reported that the Na_2SiO_3 accompanied the primary phase.

In various studies, the silica is used to prepare Na_2FeSiO_4 was usually from TEOS. It may be replaced with organic silica derived from rice husks so that the cost needed to produce Na_2FeSiO_4 becomes relatively low. According to previous studies [11,12], rice husk ash contains silica with a percentage of about 79-98% of rice husk ash weight and the silica can be extracted with a purity reaching 99%. In addition, amorphous rice husk silica is reactive, so it may be used as a raw material to prepare several silica-based materials [13]. The feasibility of silica from rice husks as raw material for making Na_2FeSiO_4 has been demonstrated by Riyanto *et al.* [14]. According to the study, the Na_2FeSiO_4 precursor was sintered at 800 ºC for 10 h and produced a crystal phase of Na_2FeSiO_4, accompanied by secondary phases Na_2SiO_3 and SiO_2. Previous studies also successfully utilized rice husk silica for fabricating several materials such as cordierite, forsterite and bituminous composite [15-18].

The high purity Na_2FeSiO_4 phase was quite challenging to obtain other phases were formed following it, even with different thermal treatments [6-10,14]. Several phases, which are usually accompany Na_2FeSiO_4 including Na_2SiO_3, Fe_3O_4 and SiO_2 [7,8,10,14]. However, these studies also mainly report limited phase composition in the qualitative analysis without informing quantitative phase composition. Furthermore, Na_2FeSiO_4 is consistently prepared at a maximum temperature of 800 ºC, as reported by Riyanto *et al.* [14]. Therefore, studies can predict the phase composition quanti-tatively in Na_2FeSiO_4 samples sintered at higher temperatures (< 800 ºC) are required to identify the phase compositions. To achieve this goal, Na_2FeSiO_4 samples were prepared by sol-gel route follwed by thermal process at 805, 810 and 815 ºC. Furthermore, the purpose of this research is to investigate the electrical properties of Na_2FeSiO_4 synthesized from rice husk silica, such as its band gap and electrical conductivity.

EXPERIMENTAL

The materials used to synthesize Na_2FeSiO_4 were rice husk, ferric nitrate nonahydrate (99%, Merck), sodium hydroxide (90%, Rp Chemical Product), citric acid monohydrate and nitric acid.

Amorphous silica extraction: A reported method was used to prepare silica powder from dried rice husks [14]. In brief, rice husks (50 g) and 500 mL of NaOH (5%) solution were mixed and then heated for 30 min in a beaker glass until a dark brown sol was obtained. The mixture was cooled for 24 h at room temperature. Afterward, it was filtered using micro-pores paper to acquire the sol and finally discard the rice husk residue. After that 10% nitric acid solution was added dropwise into the sol until the solution's pH was equal to 7 to obtain silica gel. The gel was washed thoroughly by deionized water and then subjected to thermal at 110 ºC to transform silica gel into solid. It was crushed and sieved using a 200 meshes sieve to procure fine amorphous silica powder.

Preparation of Na_2FeSiO_4 precursor: Na_2FeSiO_4 was prepared using the sol-gel method by following procedure [14]. The precursor was prepared from NaOH, ferric nitrate nona-hydrate, amorphous silica powder and citric acid monohydrate with a mole ratio of 2:1:1:1. The prepared amorphous silica powder (0.3 g) was dissolved in NaOH solution under continuous stirring at 60 ºC for 30 min followed by the addition of ferric nitrate nonahydrate solution and then citric acid was added dropwise into the solution till the pH becomes 1. The solution was refluxed at 80 ºC for 5 h before being placed into a beaker for continuous stirring at 75 ºC until the solvent was evaporated and a gel was obtained, which was finally dried at 130 ºC. Furthermore, it was ground to obtain Na_2FeSiO_4 precursor before being sintered for 10 h at 805, 810 and 815 ºC with a heat flow of 3 ºC/min.

Characterization: Nicolet iS10 Fourier transform infrared (FTIR) was used to detect the functional groups of sintered Na_2FeSiO_4 precursor samples in the wavelength range of 4000-400 cm^{-1} using KBr pallets. The phase of the sintered sample was characterized using X'Pert Powder PW 30/40 X-ray diffraction (XRD) with Cu$K\alpha$ radiation operated at 40 kV and 30 mA. The step size used was 0.02º/min with 25 range of 10-80º. The collected XRD pattern data was characterized by qualitative and quantitative analysis. The qualitative analysis was performed using QualX version 2.24 software, which is used to identify several phases present in the sample by matching experimental data with a crystallographic open database (COD) [19]. The quantitative analysis (Rietveld refinement) was carried out using the Rietica software applying the Le-Bail method. The band gap was estimated from the reflectance data in the 200-800 nm wavelength range using Shimadzu UV-2450 ultraviolet-visible diffuse reflectance spectroscopy (UV-Vis DRS) spectrophotometer. Furthermore, the band gap's value was estimated using the Kubelka-Munk theorem (eqn. 1) and the Tauc relation (eqn. 2):

$$F(R_\infty) = \frac{K}{S} = \frac{(1-R_\infty)^2}{2R_\infty} \quad (1)$$

$$[F(R_\infty)h\nu]^2 = A(h\nu - E_g) \quad (2)$$

where $F(R_\infty)$ is the Kubelka-Munk function, K is the absorption coefficient (m^2/kg), S is the scattering coefficient (m^2/kg), R_∞ is the diffuse reflectance, h is the Plank constant (6.6×10^{-34} m^2 kg/s), A is the proportionality constant (J), u is the frequency (Hz), dan E_g is the band gap energy (eV).

The cylindrical pellet was prepared by compacting 1.2 g of a sintered sample under a pressure of 78,400 KPa. The electrical conductivity of the pellet was measured using the HIOKI 3520-52 LCR meter in the frequency range of 10-1500 Hz. The conductance was converted into electrical conductivity using eqn. 3. The output measurement was conductance , which depend upon frequency.

$$s = G\frac{l}{A} \quad (3)$$

where s is the electrical conductivity (S/m), l and A are the thickness (m), G is the conductance (Siemens) and the cross-section of cylindrical pellet (m^2), respectively.

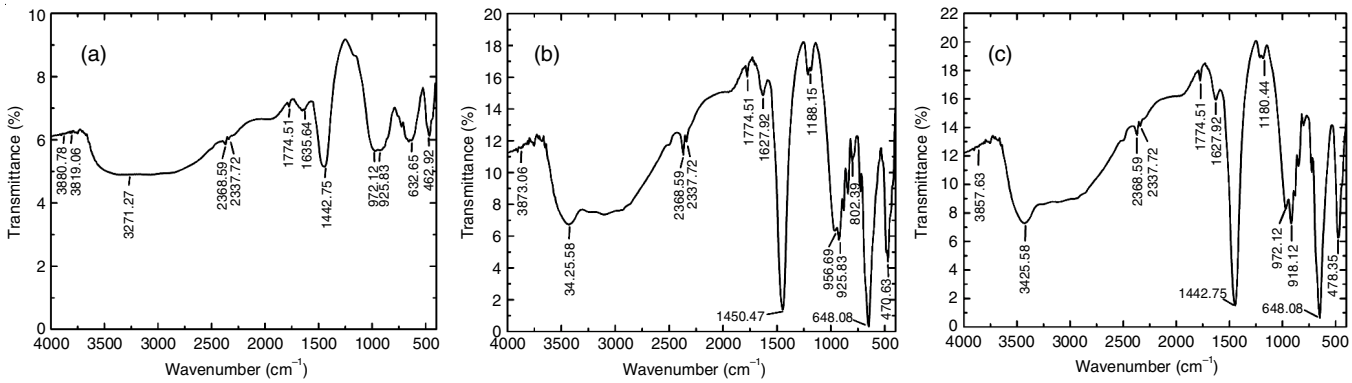

Fig. 1. FTIR spectra of samples sintered at different temperatures, (a) 805 °C, (b) 810 °C and (c) 815 °C

RESULTS AND DISCUSSION

The FTIR spectra of the samples sintered at 805, 810 and 815 ºC are depicted in Fig. 1a-c. The spectrum reveals chemical bonds related to the tetrahedral structures of NaO_4, FeO_4 and SiO_4, characterized by several absorption peaks associated with Na-O, Fe-O, Si-O and also Si-O-Si groups. The absorption peak at 462.92-478.35 cm^{-1} is associated to the Na-O group's stretch vibration [20]. The existence of Fe-O groups is indicated by absorption peaks in the range of 632.65-648.08. cm^{-1}, which is correlated with the stretching vibrations [21]. Meanwhile, the absorption peaks at 802.39 cm^{-1} and 918.12-925.83 cm^{-1} are attributed to the Si-O symmetric bending and stretching vibrations, respectively. Moreover, the absorption peak at 1188.15 cm^{-1} corresponds to the bending symmetry of the Si-O-Si groups [22-24].

The presence of absorption peaks at 1627.92-1635.64 cm^{-1} indicates the presence of bending vibrations of hydroxyl group (-OH) [22,24]. Moreover, the absorption peaks at 3271.27, 3425.58, 3880.78-3819.06 cm^{-1} are also related to the vibration of the O-H group [22,25,26]. The group normally comes from water molecules trapped in the samples or associated with the silanol group in $Si(OH)_4$ [17]. The C=O group is detected from the appearance of the absorption peak at 1774.51 cm^{-1}, while a strong absorptions at 1442.75, 2368.59 and 2337.72 cm^{-1} peak marks the presence of the C-H group [27-30]. The C=O and C-H groups possibly arise from the chelating agent citric acid monohydrate, which remained in the sample [31].

XRD studies: The experimental X-ray patterns were compared to the crystallographic databases of several polyanion compounds such as Na_2ZnSiO_4, Na_2MnSiO_4, or Na_2CaSiO_4, because the phase database of Na_2FeSiO_4 is not yet available in COD [7]. The polyanion compounds were selected as references because they resemble the crystal structure of Na_2FeSiO_4. The samples were analyzed qualitatively by matching the experimental data with a COD in the QualX program using the search-match method. The analysis reveals that the diffraction data are close to the phase database of Na_2CaSiO_4 (COD 00-101-0111). The diffraction peak indicates this match with the highest intensity at angle 2θ 33.97º, the highest peak of the Na_2FeSiO_4 phase and at 2θ of 20.64º and 45.05º, which are the typical peaks of the phase (Fig. 2). The search results also agreed with the results of previous studies [6,32], which showed that the typical peaks of Na_2FeSiO_4.

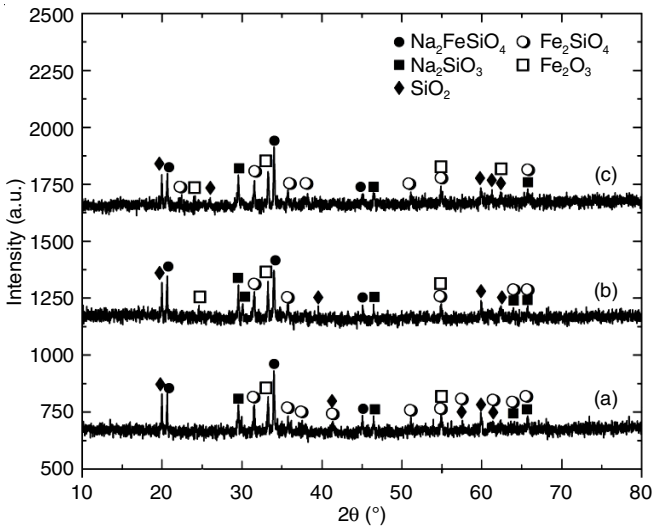

Fig. 2. Diffractogram of samples sintered at different temperatures, (a) 805 °C, (b) 810 °C and (c) 815 °C

This qualitative analysis also revealed several oxide phases, such as Na_2SiO_3, SiO_2, Fe_2O_3 and Fe_2SiO_4. The existence of Na_2SiO_3 phase is indicated by the diffraction peaks at 2θ 46.44º and 68.04º, with the highest intensity at 2θ 29.51º (COD 00-231-0858). while the central peak of SiO_2 is situated at 2θ 19.97º. Further several other diffraction peaks are related with the existence of the phase at 41.35º and 59.85º (COD 00-810-4322). The prominent peaks of the Fe_2O_3 phase are located at 33.25°, while other peaks are located at 2θ 54.91º and 62.28º (COD 01-154-6383). Meanwhile, Fe_2SiO_4 phase's prominent peak is situated at 31.52º and several other diffraction peaks associated with this phase are located at 35.74º, 41.35º, 54.91º, 57.56º and 65.72 (COD 00-100-0064). The presence of several oxide phases in each sample is well supported by FTIR studies since the phases are made up of Si-O, Si-O-Si, Na-O and Fe-O functional groups. These phases have different crystal structures and space groups. The crystal structure and space groups of each phase identified are shown in Table-1.

The qualitative phase analysis results were used as input in the Rietveld refinement analysis. The output of the Rietveld analysis of each sample is shown in Fig. 3, while the values of the refinement parameters, including R_{exp}, R_{wp} and R_p, are shown in Table-2. According to Kisi [33], the values of R_{exp}, R_{wp} and

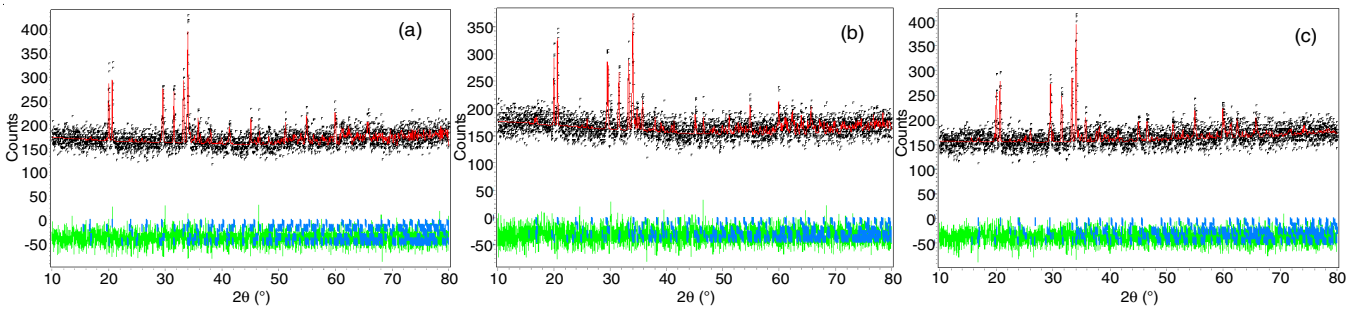

Fig. 3. XRD rietveld plot for samples sintered at different temperatures (a) 805 °C, (b) 810 °C and (c) 815 °C

TABLE-1
CRYSTAL STRUCTURE AND SPACE GROUP OF EACH PHASE

Phase	Unit cell	Space group
Na_2FeSiO_4	Cubic	P213
Na_2SiO_3	Orthorombic	C mc21
SiO_2	Tetragonal	P41212
Fe_2O_3	Trigonal	R-3c:H
Fe_2SiO_4	Orthorombic	Pbnm

TABLE-2
RIETVELD REFINEMENT PARAMETER OF EACH SAMPLE

Sample sintered (°C)	R_{wp} (%)	R_p (%)	R_{exp} (%)	GoF (%)
805	8.8	6.42	7.60	1.13
810	8.6	6.58	7.67	1.16
815	8.4	6.57	7.70	1.14

R_p for each sample have appropriate the standard. Rietveld refinement analysis is characterized by a GoF parameter less than 4% and R_{wp} less than 25% [34]. Therefore, this Rietveld analysis confirms the accuracy of the qualitative analysis results, revealing several phases, including Na_2FeSiO_4, Na_2SiO_3, SiO_2, Fe_2O_3 and Fe_2SiO_4 in the samples.

The weight percent (wt.%) of each phase in the samples is another conclusion of the Rietveld analysis. According to Table-3, the phase composition is dominated by SiO_2 and Na_2FeSiO_4, followed by Fe_2O_3, Fe_2SiO_4, Na_2SiO_3, respectively. Although the diffraction peak with the highest intensity on the diffractogram belongs to the Na_2FeSiO_4 phase and the SiO_2 phase composition is slightly more because several diffraction peaks are associated with that phase. Compared to previous study, the samples subjected to thermal higher than 800 ºC exhibit more phases than those subjected to thermal less than 800 ºC [14]. It indicates that sintering at high temperatures higher than 800 ºC triggers the crystallization of some oxide compounds and silicate derivatives. In the temperature range of 805-815 ºC, the sintering temperature increase does not cause significant changes in weight percent of the phases found in the samples. However, the volume of unit cells in each phase increases linearly with increasing sintering temperature (Table-4), which means that the distance between the atoms in the crystal structure is farther apart as the sintering temperature increases.

TABLE-3
WEIGHT PERCENT (wt.%) OF EACH PHASE FOR THE SAMPLES SINTERED AT DIFFERENT TEMPERATURES

Temp. (°C)	Na_2FeSiO_4	SiO_2	Fe_2O_3	Fe_2SiO_4	Na_2SiO_3
805	23.51	25.67	21.28	18.64	10.98
810	23.50	25.64	21.25	18.69	10.91
815	23.53	25.58	21.21	18.75	10.91

TABLE-4
UNIT CELL VOLUME (Å^3) DATA EACH PHASE FOR THE SAMPLES SINTERED AT DIFFERENT TEMPERATURES

Temp. (°C)	Na_2FeSiO_4	SiO_2	Fe_2O_3	Fe_2SiO_4	Na_2SiO_3
805	406.2763	477.4479	343.9838	306.6965	299.0868
810	408.7002	479.8727	345.5215	309.4688	301.4121
815	411.0010	480.7717	346.1445	311.3046	302.8009

The band gap values were estimated using the Kubelka-Munk theorem and the Tauc plot, as shown in Fig. 4. Tauc plot gradient intersects the *x*-axis or band gap axis at 1.84 eV, which indicated that they have identical band gap values. In the temperature range of 805-815 ºC, the increasing temperature does not significantly influence the samples' band gap

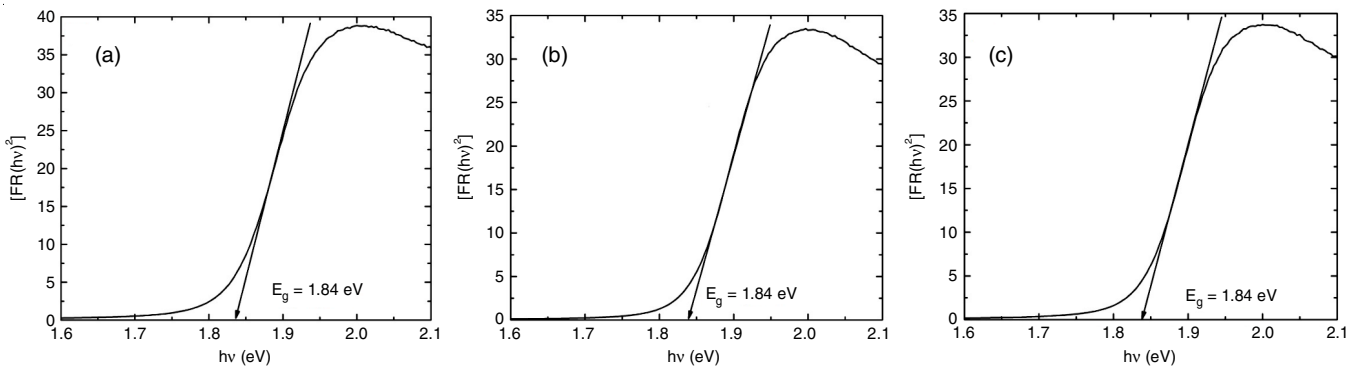

Fig. 4. Tauc plot of samples sintered at different temperatures (a) 805 °C, (b) 810 °C and (c) 815 °C

since they have a relatively similar phase composition (Table-3). Meanwhile, the electrical conductivity values revealed the considerable differences. The value of the electrical conductivity in the frequency range of 10-1500 Hz is shown in Fig. 5. The value of the electrical conductivity of each sample increases gradually with the increasing frequency following a logarithmic function. The conductivity of the samples sintered at 805, 810 and 815 ºC was $0.10 \times 10^{-5} - 6.92 \times 10^{-5}$ S/m, $0.25 \times 10^{-5} - 7.04 \times 10^{-5}$ S/m and $1.90 \times 10^{-5} - 20.83 \times 10^{-5}$ S/m, respectively. The tendency of increasing the electrical conductivity as the sintering temperature increases is strongly suspected to be related to the rise in the volume of each unit cell, as shown in Table-4. The increase in the unit cell volume causes the distance between the atoms to be further apart. As a result, the bonds between atoms are getting weaker so that electrons can be released with lower energy to be free electrons [35,36].

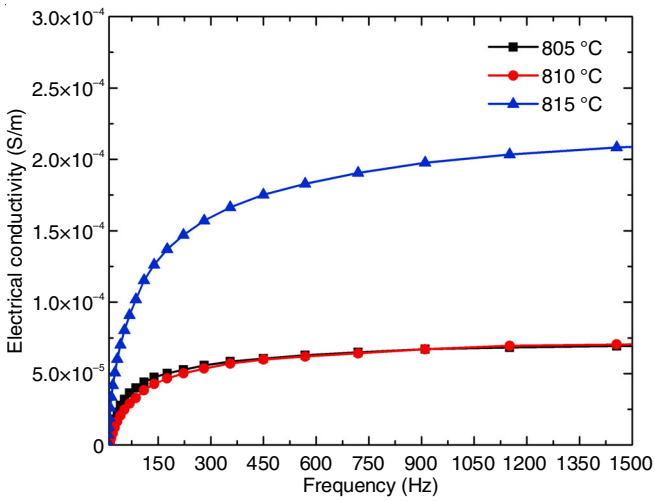

Fig. 5. Electrical conductivity at range frequency of 10-1500 Hz of samples sintered at different temperatures

Conclusion

This study demonstrated that Na_2FeSiO_4 precursor derived from rice husk silica and annealed at 805-815 ºC produce some phases, such as Na_2FeSiO_4, SiO_2, Fe_2O_3, Fe_2SiO_4 and $NaSiO_3$. In the studied temperature range, the weight percent of the phases and band gap of samples did not significantly differ from one to the other. However, it's unit cell volume increased with increasing sintering temperature, followed by increasing its electrical conductivity.

ACKNOWLEDGEMENTS

The authors express their gratitude to the Universitas Lampung for providing the financial support for this research through a fundamental research grant (contract no. 654/UN26.21/PN/2022).

CONFLICT OF INTEREST

The authors declare that there is no conflict of interests regarding the publication of this article.

REFERENCES

1. C. Eames, A.R. Armstrong, P.G. Bruce and M.S. Islam, *Chem. Lett.*, **24**, 2155 (2012); https://doi.org/10.1021/cm300749w
2. P. Vajeeston and H. Fjellvag, *RSC Adv.*, **7**, 16843 (2017); https://doi.org/10.1039/C6RA26555C
3. P. Sivaraj, K.P. Abhilash, B. Nalini, P. Balraju, S.K. Yadav, S. Jayapandi and P. Christopher Selvin, *Ionics*, **25**, 2041 (2019); https://doi.org/10.1007/s11581-018-2685-1
4. Z. Ye, X. Zhao, S. Li, S. Wu, P. Wu, M.C. Nguyen, J. Guo, J. Mi, Z. Gong, Z.-Z. Zhu, Y. Yang, C.-Z. Wang and K.-M. Ho, *Electrochim. Acta*, **212**, 934 (2016); https://doi.org/10.1016/j.electacta.2016.07.073
5. S. Guo, J. Li, Q. Xu, Z. Ma and H. Xue, *J. Power Sources*, **361**, 285 (2017); https://doi.org/10.1016/j.jpowsour.2017.07.002
6. S. Li, J. Guo, Z. Ye, X. Zhao, S. Wu, J.-X. Mi, C.-Z. Wang, Z. Gong, M.J. McDonald, Z. Zhu, K.-M. Ho and Y. Yang, *ACS Appl. Mater. Interfaces*, **8**, 17233 (2016); https://doi.org/10.1021/acsami.6b03969
7. Y. Kee, N. Dimov, A. Staykov and S. Okada, *Mater. Chem. Phys.*, **171**, 45 (2016); https://doi.org/10.1016/j.matchemphys.2016.01.033
8. K. Kaliyappan and Z. Chen, *Electrochim. Acta*, **283**, 1384 (2018); https://doi.org/10.1016/j.electacta.2018.07.034
9. Z. Feng, M. Tang and Z. Yan, *Ceram. Int.*, **44**, 22019 (2018); https://doi.org/10.1016/j.ceramint.2018.08.186
10. W. Guan, B. Pan, P. Zhou, J. Mi, D. Zhang, J. Xu and Y. Jiang, *ACS Appl. Mater. Interfaces*, **9**, 22369 (2017); https://doi.org/10.1021/acsami.7b02385
11. Y.E. Simsek, *Acta Phys. Polineca A*, **132(3-II)**, 1002 (2017); https://doi.org/10.12693/APhysPolA.132.1002
12. R.A. Bakar, R. Yahya and S.N. Gan, *Procedia Chem.*, **19**, 189 (2016); https://doi.org/10.1016/j.proche.2016.03.092
13. N.N. Ngoc, L.X. Thanh, L.T. Vinh and B.T. Van Anh, *Vietnam J. Chem.*, **56**, 730 (2018); https://doi.org/10.1002/vjch.201800079
14. A. Riyanto, S. Sembiring, A.R. Amalia, A. Astika and R. Marjunus, *J. Phys. Conf. Ser.*, **1572**, 012003 (2020); https://doi.org/10.1088/1742-6596/1572/1/012003
15. S. Sembiring, W. Simanjuntak, R. Situmeang, A. Riyanto and P. Karo-Karo, *J. Asian Ceram. Soc.*, **5**, 186 (2017); https://doi.org/10.1016/j.jascer.2017.04.005
16. S. Sembiring, W. Simanjuntak, R. Situmeang and A. Riyanto, *J. Ceram. Silik.*, **62**, 163 (2018); https://doi.org/10.13168/cs.2018.0008
17. S. Sembiring, A. Riyanto, W. Simanjuntak and R. Situmeang, *Orient. J. Chem.*, **33**, 1828 (2017); https://doi.org/10.13005/ojc/330427
18. S. Sembiring, A. Riyanto, R. Situmeang and Z. Sembiring, *J. Ceram. Silik.*, **63**, 277 (2019); https://doi.org/10.13168/cs.2019.0021
19. A. Altomare, C. Cuocci, C. Giacovazzo, A. Moliterni and R. Rizzi, *J. Appl. Cryst.*, **41**, 815 (2008); https://doi.org/10.1107/S0021889808016956
20. V.S. Rangasamy, S. Thayumanasundaram and J. Locquet, *Electrochim. Acta*, **276**, 102 (2018); https://doi.org/10.1016/j.electacta.2018.04.166
21. R. Jain, V. Luthra, M. Arora and S. Gokhale, *J. Supercond. Nov. Magn.*, **32**, 325 (2019); https://doi.org/10.1007/s10948-018-4717-5
22. K.S. Hui and C.Y.H. Chao, *J. Hazard. Mater.*, **137**, 1135 (2006); https://doi.org/10.1016/j.jhazmat.2006.03.050.
23. M. Sheykhan, A. Yahyazadeh and L. Ramezani, *Mol. Catal.*, **435**, 166 (2017); https://doi.org/10.1016/j.mcat.2017.03.032
24. U. Kalapathy, *Bioresour. Technol.*, **73**, 257 (2000); https://doi.org/10.1016/S0960-8524(99)00127-3
25. U.O. Aroke, A. Abdulkarim and R.O. Ogubunka, *ABTU J. Environ. Technol.*, **6**, 42 (2013).

26. A. Célino, O. Gonçalves, F. Jacquemin and S. Fréour, *Cabohydr. Polym.*, **101**, 163 (2014); https://doi.org/10.1016/j.carbpol.2013.09.023
27. C. Ma, C. Yin, Y. Fan, X. Yang and X. Zhou, *J. Mater. Sci.*, **54**, 9372 (2019); https://doi.org/10.1007/s10853-019-03585-7
28. J. Zhuang, M. Li, Y. Pu, A.J. Ragauskas and C.G. Yoo, *Appl. Sci.*, **10**, 4345 (2020); https://doi.org/10.3390/app10124345
29. A.B.D. Nandiyanto, R. Oktiani and R. Ragadhita, *Indones. J. Sci. Technol.*, **4**, 97 (2019); https://doi.org/10.17509/ijost.v4i1.15806
30. M.H.S. Abadi, A. Delbari, Z. Fakoor and J. Baedi, *J. Ceram. Sci. Technol.*, **46**, 41 (2015); https://doi.org/10.4416/JCST2014-00028
31. P. Sivaraj, B. Nalini, K.P. Abhilash, D. Lakshmi, P.C. Selvin and P. Balraju, *J. Alloys Compd.*, **740**, 1116 (2018); https://doi.org/10.1016/j.jallcom.2018.01.051
32. B. Ali, A. Ur-Rehman, F. Ghafoor, M.I. Shahzad, S.K. Shah and S.M. Abbas, *J. Power Sources*, **396**, 467 (2018); https://doi.org/10.1016/j.jpowsour.2018.06.049
33. E.H. Kisi, *Mater Forum*, **18**, 135 (1994).
34. S. Sembiring, W. Simanjuntak, R. Situmeang, A. Riyanto and K. Sebayang, *Ceram. Int.*, **42**, 8431 (2016); https://doi.org/10.1016/j.ceramint.2016.02.062
35. R. Dalven, *Phys. Rev. B*, **8**, 6033 (1973); https://doi.org/10.1103/PhysRevB.8.6033
36. T.D. Malevu and R.O. Ocaya, *Int. J. Electrochem. Sci.*, **10**, 1752 (2015).